

Infrared optical absorption of Fröhlich polarons in metal halide perovskites

Yu Cui(崔钰), Xiao-Yi Liu(刘晓逸), Xu-Fei Ma(马旭菲), Jia-Pei Deng(邓加培), Yi-Yan Liu(刘怡言), and Zi-Wu Wang(王子武)

Citation: Chin. Phys. B, 2023, 32 (**9**): 097102. DOI: 10.1088/1674-1056/aca7f0
Journal homepage: http://cpb.iphy.ac.cn; http://iopscience.iop.org/cpb

What follows is a list of articles you may be interested in

Coherent interaction and action-counteraction theory in small polaron systems, and ground state properties

Zhi-Hua Luo(罗质华) and Chao-Fan Yu(余超凡)
Chin. Phys. B, 2022, 31 (**11**): 117104. DOI: 10.1088/1674-1056/ac67c1

Dynamic recombination of triplet excitons in polymer heterojunctions

Ya-Dong Wang(王亚东), Jian-Jun Liu(刘建军), Xi-Ru Wang(王溪如), Yan-Xia Liu(刘艳霞), and Yan Meng(孟艳)
Chin. Phys. B, 2020, 29 (**11**): 117101. DOI: 10.1088/1674-1056/ab9c13

Magnetpolaron effect in two-dimensional anisotropic parabolic quantum dot in a perpendicular magnetic field

Kang-Kang Ju(居康康), CuiXian Guo(郭翠仙), Xiao-Yin Pan(潘孝胤)
Chin. Phys. B, 2017, 26 (**9**): 097103. DOI: 10.1088/1674-1056/26/9/097103

Temperature and hydrogen-like impurity effects on the excited state of the strong coupling bound polaron in a CsI quantum pseudodot

Jing-Lin Xiao(肖景林)
Chin. Phys. B, 2017, 26 (**2**): 027104. DOI: 10.1088/1674-1056/26/2/027104

Crossover of large to small radius polaron in ionic crystals

M I Umo
Chin. Phys. B, 2016, 25 (**11**): 117104. DOI: 10.1088/1674-1056/25/11/117104

Infrared optical absorption of Fröhlich polarons in metal halide perovskites

Yu Cui(崔钰), Xiao-Yi Liu(刘晓逸), Xu-Fei Ma(马旭菲),
Jia-Pei Deng(邓加培), Yi-Yan Liu(刘怡言), and Zi-Wu Wang(王子武)†

Tianjin Key Laboratory of Low Dimensional Materials Physics and Preparing Technology, Department of Physics, School of Science, Tianjin University, Tianjin 300354, *China*

(Received 24 October 2022; revised manuscript received 24 November 2022; accepted manuscript online 2 December 2022)

The formation of Fröhlich polarons in metal halide perovskites, arising from the charge carrier–longitudinal optical (LO) phonon coupling, has been proposed to explain their exceptional properties, but the effective identification of polarons in these materials is still a challenging task. Herein, we theoretically present the infrared optical absorption of Fröhlich polarons based on the Huang–Rhys model. We find that multiphonon overtones appear as the energy of the incident photons matches the multiple LO phonons, wherein the average phonon number of a polaron can be directly evaluated by the order of the strongest overtone. These multiphonon structures sensitively depend on the scale of electronic distribution in the ground state and the dimensionality of the perovskite materials, revealing the effective modulation of competing processes between polaron formation and carrier cooling. Moreover, the order of the strongest overtone shifts to higher ones with temperature, providing a potential proof that the carrier mobility is affected by LO phonon scattering. The present model not only suggests a direct way to verify Fröhlich polarons but also enriches our understanding of the properties of polarons in metal halide perovskites.

Keywords: metal halide perovskites, polaron, Huang–Rhys factor

PACS: 71.38.–k **DOI:** 10.1088/1674-1056/aca7f0

1. Introduction

The formation of Fröhlich polarons (or large polarons) originates from the coupling between a macroscopic electronic field induced by the polar optical phonon modes in a solid and a charge carrier. Such polarons are also called special carriers dressed by the 'phonon cloud' (the induced nuclear polarization), reflected by the average phonon number.[1–3] This type of polaron has aroused much interest in relation to metal halide perovskites (MHPs) because it has been used to unlock key puzzles regarding their exceptional properties,[4–7] such as their moderate carrier mobility, large carrier diffusion length, long carrier lifetime and high defect tolerance. Therefore, the identification of this type of polaron in MHPs has become a crucial problem in both experimental and theoretical studies.

In the past few years, the formation of Fröhlich polarons in perovskite materials has been probed in spectral measurements: following the polaron formation dynamics in time-resolved optical Kerr effect spectroscopy,[8] ultrafast terahertz (THz) spectroscopy[9] as well as time-resolved two-photon photoemission and transient reflectance spectroscopies;[10] examining Pb–I structural dynamics in time-domain Raman spectroscopy;[11] and studying the electronic structure in angle-resolved photoelectron spectroscopy.[12] On the other hand, large polarons can be also investigated by other measurements such as the mobility of charge carrier scaling with temperature in transport[13] and Hall effect measurements.[14] From a theoretical perspective, large polarons forming predominantly from the distortion or deformation of the crystal structure with first-principles calculations have also been widely studied.[15–17] Despite the experimental and theoretical evidence confirming the formation of large polarons in perovskite materials, detailed knowledge and direct distinction of the 'phonon cloud' of a polaron, which is the crucial ingredient determining the nature of the polaron, are not well understood to date.

In this paper, we theoretically study the infrared optical absorption of Fröhlich polarons in three-dimensional (3D) and two-dimensional (2D) MHP materials stemming from the strong electron–longitudinal optical (LO) phonon mode coupling. We find that the 'phonon cloud' of a polaron can be directly reflected by the multiple LO phonon structure of the optical absorption spectra, in which the average phonon numbers described very well by the dimensionless Huang–Rhys (HR) factor are directly linked to the order of the strongest absorption peak. Moreover, the strongest absorption peak shifts to the higher order with decreasing electronic distribution radius in the ground state, indicating that the range of the electronic distribution plays an important role in determining the electron–LO phonon coupling. Meanwhile, the temperature dependence of the polaron absorption processes is also discussed.

†Corresponding author. E-mail: wangziwu@tju.edu.cn

© 2023 Chinese Physical Society and IOP Publishing Ltd

2. Theoretical method

As depicted in Fig. 1, the absorption of light by polarons can be described as follows: when the incident photon energy $\hbar\omega$ matches the energy of the multiple LO phonons $p\hbar\omega_{\rm LO}$, the polaron system will undergo transitions from the ground state $|\Psi_i\rangle = |\psi_{1s}\rangle|\chi_{in'_{\boldsymbol{q}}}\rangle$ with energy E_i towards a series of excited states $|\Psi_f\rangle = |\psi_{1s}\rangle|\chi_{fn_{\boldsymbol{q}}}\rangle$ with energy $E_f = E_i + p\hbar\omega_{\rm LO}$. $|\psi_{1s}\rangle$ is the ground state of the polaron and $|\chi_{in'_{\boldsymbol{q}}}\rangle$ ($|\chi_{fn_{\boldsymbol{q}}}\rangle$) is the initial (final) lattice wave function, where $n'_{\boldsymbol{q}}$ ($n_{\boldsymbol{q}}$) is the occupation number for phonons with the wave vector $\boldsymbol{q}$. Note that the optical absorption discussed here is one-polaron behavior rather than that of a many-polaron gas. As is typical of multiphonon transition process, it is excellently described by the HR model.[18–21] By means of this well-known model, the probability of optical absorption for light with frequency ω can be expressed as[22–24]

$$\mathcal{F}(\hbar\omega) = \sum_f \frac{4\pi^2 e^2\hbar\omega}{3m^2\hbar^2\varepsilon c}|\langle\psi_{1s}|\boldsymbol{r}|\psi_{1s}\rangle|^2\left|\langle\chi_{fn_{\boldsymbol{q}}}|\chi_{in'_{\boldsymbol{q}}}\rangle\right|^2 \times\delta(E_f - E_i - \hbar\omega), \tag{1}$$

where e is the charge carrier, $\hbar\omega$ is the photon energy, m is the effective mass of the polaron, ε is the permittivity, c is the velocity of light and $\boldsymbol{r}$ represents the position variables for polaron. Here the spatial average $\langle|\boldsymbol{r}_{if}\cdot\boldsymbol{E}_0|^2\rangle = |\boldsymbol{r}_{if}|^2|\boldsymbol{E}_0|^2/3$ and the relation $\hbar\omega = \varepsilon c|\boldsymbol{E}_0|^2/(8\pi)$ for the electronic dipole approximation have been used.[25]

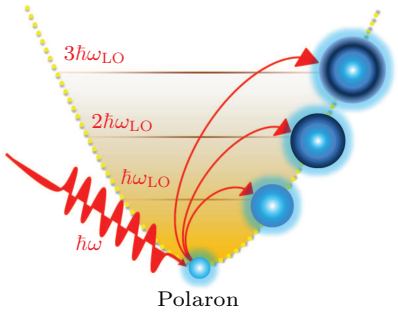


Fig. 1. Schematic diagram of optical absorption of the polaron, where $\hbar\omega$ is the incident photon energy and $\hbar\omega_{\rm LO}$ is the longitudinal optical (LO) phonon energy.

For the ground state of polaron, a Gaussian wave function is considered:[26]

$$\psi^{\lambda}_{1s}(r) = \mathcal{C}_\lambda \exp\left(-\frac{r^2}{4a_0^2}\right), \tag{2}$$

where the normalization constant $\mathcal{C}_\lambda = [1/(\sqrt{2\pi}a_0)]^{3/2}$ for $\lambda = 3$D and $\mathcal{C}_\lambda = 1/(\sqrt{2\pi}a_0)$ for $\lambda = 2$D ($\lambda = 3$D and $\lambda = 2$D represent the 3D and 2D materials, respectively). Figure S1 in the supplemental materials shows the corresponding crystal structure for 3D and 2D MHPs, where the 2D MHP has distinct quantum confinement on the z-axis. a_0 represents the radius of electronic distribution in the ground state. Upon substitution of Eq. (2), Eq. (1) will be simplified as

$$\mathcal{F}^{\lambda}(\hbar\omega) = \sum_f \Re_\lambda a_0^2\hbar\omega\left|\langle\chi_{fn_{\boldsymbol{q}}}|\chi_{in'_{\boldsymbol{q}}}\rangle\right|^2 \times\delta(E_f - E_i - \hbar\omega). \tag{3}$$

$\Re_{\rm 3D} = 32\pi e^2/(3m^2\hbar^2\varepsilon c)$ and $\Re_{\rm 2D} = 2\pi^3 e^2/(3m^2\hbar^2\varepsilon c)$ are the optical constants. The overlap between the initial $|\chi_{in'_{\boldsymbol{q}}}\rangle$ and the final $|\chi_{fn_{\boldsymbol{q}}}\rangle$ lattice vibrations produced by the lattice displacement occurs during the transition process, which is responsible for the multiple phonon structure, linked to the electron–phonon coupling. Substituting the expression for the square of the overlap integral $\left|\langle\chi_{fn_{\boldsymbol{q}}}|\chi_{in'_{\boldsymbol{q}}}\rangle\right|^2$, shown in the supplemental materials, into Eq. (3), we finally convert the optical absorption spectra of polarons involving the participation of p phonons at finite temperature into

$$\mathcal{F}^{\lambda}(\hbar\omega) = \Re_\lambda a_0^2\hbar\omega\left(\frac{\bar{n}_T+1}{\bar{n}_T}\right)^{p/2}\exp[-S^\lambda(2\bar{n}_T+1)] \times I_p(2S^\lambda\sqrt{\bar{n}_T(\bar{n}_T+1)}) \times\exp\left[-\frac{(\hbar\omega - p\hbar\omega_{\rm LO})^2}{2\sigma^2}\right]. \tag{4}$$

LO phonons are mainly taken into account because they couple with the charge carriers in the Fröhlich mechanism as the main source of lattice distortion for MHP materials not only in theory but also in experiments.[27–30] $\bar{n}_T = 1/(\mathrm{e}^{\hbar\omega_{\rm LO}/k_{\rm B}T} - 1)$ is the phonon number occupation function where $k_{\rm B}$ and $\hbar\omega_{\rm LO}$ are the Boltzmann constant and LO phonon energy, respectively, and I_p is the pth-order imaginary argument Bessel function with the phonon number p. σ represents the line-width of the phonon overtone. The strength of electron–phonon coupling has been characterized using the HR factor S^λ, which plays a nontrivial role in determining multiphonon processes. In the Fröhlich mechanism,[26,31,32] the HR factor can be calculated by

$$S^\lambda = \sum_{\boldsymbol{q}}\ell_\lambda(q)\left(\frac{\hbar}{2m^*\omega_{\rm LO}}\right)^{1/2}\left|\int\psi^{\lambda*}_{1s}(r)\,\mathrm{e}^{\mathrm{i}\boldsymbol{q}\cdot\boldsymbol{r}}\psi^{\lambda}_{1s}(r)\,\mathrm{d}\boldsymbol{r}\right|^2, \tag{5}$$

where $\ell_{\rm 3D}(q) = 4\pi\alpha/(Vq^2)$ and $\ell_{\rm 2D}(q) = 2\pi\alpha/(Aq)$. The detailed derivations for the HR factor, charge carrier–LO phonon coupling, the corresponding definition and expression of parameters are shown in the supplemental materials. In the numerical calculation processes, we choose typical MHPs $CH_3NH_3PbI_3$ ($MAPbI_3$), $CH_3NH_3PbBr_3$ ($MAPbBr_3$) and $CH_3NH_3PbCl_3$ ($MAPbCl_3$) as examples to discuss the optical absorption processes of the polaron. The line-width of the phonon overtone is usually around a few meV,[2] and throughout this paper the line-width $\sigma = 3$ meV is assumed. The adopted values of other parameters for the three types of materials are shown in Table 1, and are measured by temperature-dependent photoluminescence and far-infrared spectroscopy.[33,34]

Table 1. The adopted parameters for the theoretical calculations ($m_0 = 9.1 \times 10^{-31}$ kg is the free electron mass).

Parameter	$MAPbI_3$	$MAPbBr_3$	$MAPbCl_3$
LO phonon energy ($\hbar\omega_{LO}$)	11.5 meV[33]	15.3 meV[33]	27.9 meV[34]
Coupling constant (α)	1.72[34]	1.69[34]	2.17[34]
Effective mass (m^*)	$0.104m_0$[34]	$0.117m_0$[34]	$0.2m_0$[34]
Polaron radius (R_0)	51 Å[34]	43 Å[34]	27 Å[34]

3. Results and discussion

The HR factor was originally proposed by Huang and Rhys for F-centers in ionic crystals in 1950;[18] it denotes the average phonon numbers around F-centers, reflecting the magnitude of lattice distortion arising from the strong coupling between electronic states and lattice vibrations (phonons). Herein, the HR factor is invoked to describe the 'phonon cloud' of the polaron with relaxation energy $S^{\lambda}\hbar\omega_{LO}$. The dependence of the HR factor on the electronic distribution radius in the ground state in different dimensionalities is shown in Figs. 2(a) and 2(b) for $MAPbI_3$ and $MAPbBr_3$, respectively. One can see that the HR factor increases from 3D to 2D, stemming from that both the reduced dielectric screening and increased degree of quantum confinement are held responsible for the enhancement of electron–phonon coupling. On the other hand, the HR factor exhibits a negative correlation with a_0. But the HR factor varies smoothly as a_0 exceeds $0.6R_0$ (R_0 being the polaron radius). This indicates that outside this region the localization feature of electrons has little effect on electron–phonon coupling. Numerous researchers have calculated the formation energy of large polarons. The obtained values range are 12 meV for 3D $MAPbI_3$ and 16±2 meV for 3D $MAPbBr_3$ in a tight-binding model fitted from the first-principles calculation and temperature-dependent absorption spectroscopy,[35,36] respectively. These numerical values are in good agreement with the relaxation energy $S^{3D}\hbar\omega_{LO} \approx 13.8$ meV for 3D $MAPbI_3$ and $S^{3D}\hbar\omega_{LO} \approx 18.2$ meV for 3D $MAPbBr_3$ at $a_0 \geq 0.6R_0$, implying that the formation energy can be well described by the relaxation energy. As for 2D perovskite species, although there is little direct information about polarons in the experiments, the discoveries of 2D exciton polarons and self-trapped excitons reveal significant polaronic character.[37–40] The numerical values of HR factors for 2D perovskites in Fig. 2 are expected to provide insight for the identification of these quasiparticles. The calculation of relaxation energy can indirectly evaluate the carrier lifetime (carrier lifetime is proportional to the strength of charge carrier–phonon coupling[41]) and thus provide a reference for the selection of more suitable materials for photovoltaic devices.[42] Similar results are also obtained for $MAPbCl_3$ in Fig. S2. In addition, it has been shown that the HR factor in $MAPbBr_3$ is smallest in these three types of MHP. This is ascribed to the fact that distortion of the Pb–Br bond is more difficult than that of the Pb–I and Pb–Cl bonds determined by the bond length, which is reflected by the coupling parameter α listed in Table 1. We note that the effective phonon modes and relaxation energy could be obtained from first-principles calculations,[43–45] gaining the more accurate evaluations for the HR factor. Our results will also provide an important theoretical reference for these calculations.

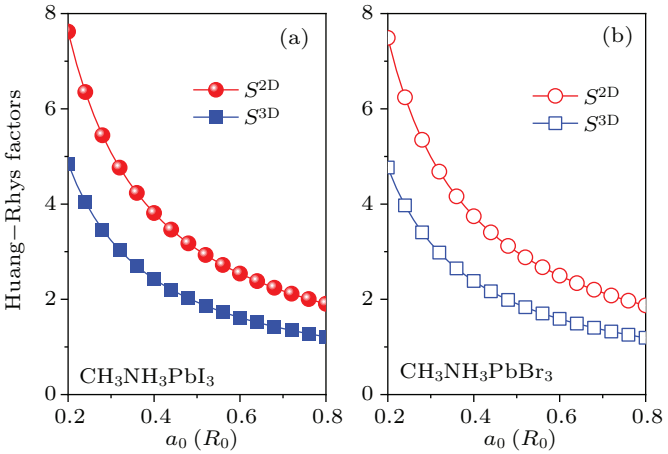


Fig. 2. Huang–Rhys (HR) factors in $CH_3NH_3PbI_3$ (a) and $CH_3NH_3PbBr_3$ (b) as a function of the electronic distribution radius in the ground state for different dimensionalities. S^{2D} and S^{3D} represent HR factors in two- and three-dimensional perovskite materials, respectively.

On the basis of these theoretical values for the HR factor, the optical absorption spectra of polarons for $MAPbI_3$ and $MAPbBr_3$ are plotted in Fig. 3 for different electronic distribution radii in the ground state, at $T = 77$ K. We first give a detailed discussion of the spectra for $MAPbI_3$. In Fig. 3(a), energy resonance absorption will occur when the energy of the incident photon matches that of the multiple LO phonons, showing multiphonon overtones in the infrared (long-wavelength) region of the spectra, where the strongest overtone corresponds to the most probable state of a polaron. The intensities of the overtones follow an asymmetric Gaussian distribution, in agreement with previous experimental measurements.[9,46] Comparison with the HR factors in Fig. 2 shows that the order of the strongest overtone p_{max} satisfies the condition of $p_{max} \approx S^{3D} + 0.7$, such as $S^{3D} \approx 2.42$ corresponding to $p_{max} = 3$ at $a_0 = 0.4R_0$, but the condition shifts to $p_{max} \approx S^{2D} + 1$ for the 2D perovskites, such as $S^{2D} \approx 3.81$ corresponding to $p_{max} = 5$ at $a_0 = 0.4R_0$, which is consistent with our previous results.[47,48] According to our simulation, the curves $S^{3D} + 0.7$ and $S^{2D} + 1$ are fitted well with p_{max} for 3D and 2D MHPs, as shown in Fig. S7. This means that the average phonon number of polarons can be estimated directly from the absorption spectra. This significant outcome can be used to explain the overtones along with a linear decay from the first to the higher orders in multiphonon Raman scattering and THz time-dominant spectroscopy for $CsPbBr_3$ ($S^{3D} = 0.39$).[30] The pronounced redshift behaviors for the position of the spectral weight with the increase in electron

localization are shown, specifically manifested in Fig. 3(a) as: (1) the number of the observable overtones reduces from seven at $a_0 = 0.4R_0$ to five at $a_0 = 0.8R_0$; (2) the most probable state transits from the third order at $a_0 = 0.4R_0$ to the second order at $a_0 = 0.8R_0$. These phenomena are direct reflections of the variation in electron–phonon coupling (HR factor) linked to charge carrier localization, showing the polaron to be more stable or more easily taken off the phonon dressing. Similar trends are also obtained for $MAPbBr_3$ (in Figs. 3(b) and 3(d)) and $MAPbCl_3$ (in Fig. S3). Recently, several experiments have proved that large polaron formation drastically suppresses the cooling of hot carriers.[10,49–51] For instance, an envelope of a Cs_4PbBr_6 lattice shell was provided over $CsPbBr_3$ nanocrystals.[51] The enhanced strength of the electron–phonon coupling in such shell material facilitates the formation of polarons with a large relaxation energy, and thus depresses the carrier cooling process. It is, therefore, concluded that if more phonon overtones appear in the infrared optical absorption measurements of perovskite materials, the polaron effect will be more pronounced, which could serve as a criterion for judging whether these perovskites materials are suitable for potential applications in photovoltaic (preferring a strong polaron effect) or photoelectronic (demanding fast carrier cooling) devices.

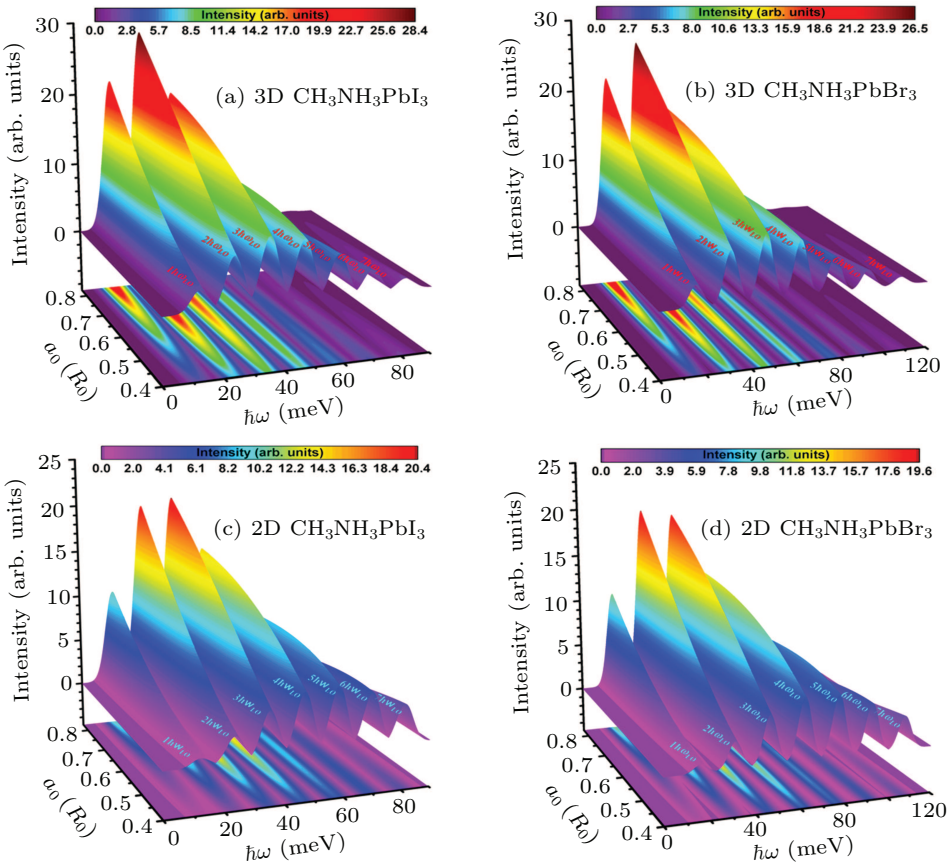


Fig. 3. Multiple LO phonon infrared optical absorption spectra in 3D $CH_3NH_3PbI_3$ (a), 3D $CH_3NH_3PbBr_3$ (b), 2D $CH_3NH_3PbI_3$ (c) and 2D $CH_3NH_3PbBr_3$ (d) for different electronic distribution radii in the ground state, at $T = 77$ K.

The temperature dependences of optical absorption in 3D $MAPbI_3$, 3D $MAPbBr_3$ and 3D $MAPbCl_3$ are shown in Figs. 4(a), 4(b) and S4, respectively. These multiphonon overtones can be divided into two regions: the low-order region including the overtones in the range of $1 \leq p \leq S^{3D} + 2$ and the high-order region comprising the rest of the overtones. In the former region, the intensities of overtones decrease monotonically with temperature. On the contrary, the latter region shows the opposite variational trends and even much higher orders of overtones will be thermally activated. This can be explained by more thermally activated LO phonons becoming available with temperature, resulting in (1) the polaron states with more phonons are prone to reach the most probable states and (2) the orders of overtones increase. The blueshift of the most probable states leads to a shift of the whole absorption spectrum towards a higher energy, showing the downward trend of the relative probability in the low-order region and the upward trend for the high-order region, as given in Fig. S5. More importantly, the polaron dressed by more thermally activated LO phonons indicates that the polaron effects are actively strengthened at higher temperature. In perovskite materials, the long carrier diffusion length does not imply a high charge carrier mobility,[8,12,36,52] yet a detailed understanding of its fundamental mechanisms is still outstanding. Accord-

ing to our theoretical study, the polarons become significantly 'heavier' with temperature because of the blueshift of the spectra mentioned above, which is not beneficial to transport, especially at room temperature. Thus this provides a potential explanation for the moderate carrier mobility in perovskites, which supports the theoretical predictions about LO phonon mode scattering influencing mobility.[34,53] Therefore, it may be more appropriate to elucidate the effective mobility by the polaron model in perovskite materials.[34,36,54–56] In turn, the measurements of the carrier mobility in experiments could also track the path of polarons.[57] It is additionally revealed that the overtones retain a stable outline even at room temperature, implying that polaron states have a very robust lifetime, which will benefit not only experimental observation but also the potential exploitation of polaron properties in perovskite materials. However, there is a prominent distinction for the peaks of overtones with temperature for these three types of material, the details of which are shown in Fig. S6. The variation of the slope indicates that the thermodynamic stability of polarons decreases in the sequence Cl>Br>I. As a result, the stability of polarons for MHP materials could suggest application potential in photovoltaics. Finally, we must emphasize that: (1) these perovskite materials undergo two structural phase transitions with temperature, which influence the strength of the electron–phonon coupling and phonon energy;[58–60] (2) the rotation of the organic monovalent cation and its coupling with the surrounding inorganic framework affects MHP optoelectronic properties.[61,62] These effects are not taken into account in the present paper.

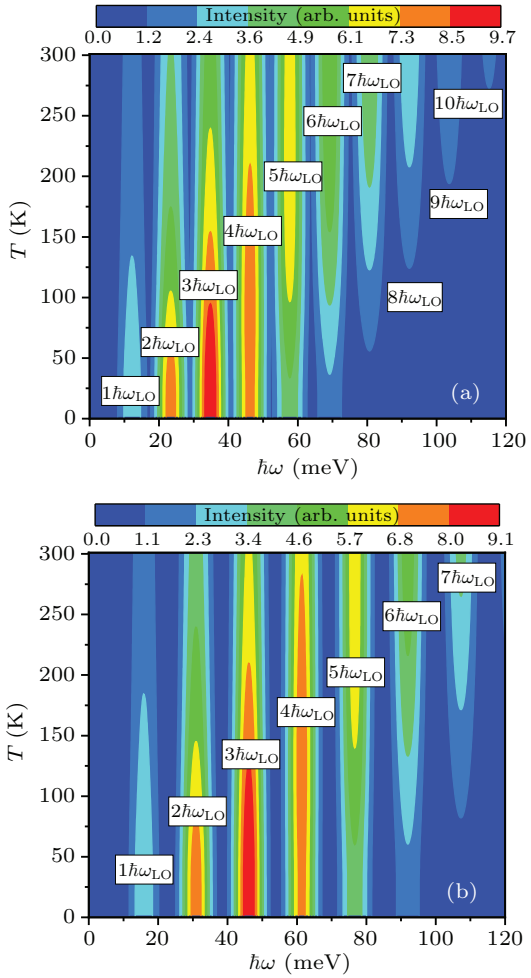


Fig. 4. The temperature dependences of multiple LO phonon structures for the optical absorption spectra in 3D $MAPbI_3$ (a) and 3D $MAPbBr_3$ (b), respectively, at $a_0 = 0.4R_0$.

4. Conclusion

In summary, we theoretically study the infrared optical absorption spectroscopy of Fröhlich polarons in metal halide perovskites. We find that: (1) the multiphonon structure can be used as the fingerprint of the polaron, where the average phonon number in the 'phonon cloud' of the polaron is reflected by the order of the strongest overtone in the absorption spectra; (2) the multiphonon structure sensitively depends on both the dimensionality of the materials and the charge carrier localization, elucidating how competing processes between polaron formation and carrier cooling are controlled, enabling more efficient design of photovoltaic and photoelectronic devices; (3) the 'phonon cloud' around the polaron will become larger as the temperature increases and thus affect the carrier mobility, especially at room temperature, which is consistent with the experimental measurements; (4) infrared optical absorption spectra for MHPs are an easy and effective method, reflecting charge carrier–phonon coupling and ensuring that new materials for energy innovation are designed rationally and appropriately to specific applications.

Acknowledgement

Project supported by the National Natural Science Foundation of China (Grant Nos. 11674241 and 12174283).

References

[1] Mishchenko A S, Prokof'ev N V, Sakamoto A and Svistunov B V 2000 *Phys. Rev. B* **62** 6317
[2] Devreese J T 2007 *J. Phys.: Condens. Matter* **19** 255201
[3] Devreese J T and Alexandrov A S 2009 *Rep. Prog. Phys.* **72** 066501
[4] Miyata K, Atallah T L and Zhu X Y 2017 *Sci. Adv.* **3** e1701469
[5] Lan Y, Dringoli B J, Valverde-Chávez D A, Ponseca Jr C S, Sutton M, He Y, Kanatzidis M G and Cooke D G 2019 *Sci. Adv.* **5** eaaw5558
[6] Mahata A, Meggiolaro D and Angelis F D 2019 *J. Phys. Chem. Lett.* **10** 1790
[7] Ghosh D, Welch E, Neukirch A J, Zakhidov A and Tretiak S 2020 *J. Phys. Chem. Lett.* **11** 3271
[8] Miyata K, Meggiolaro D, Trinh M T, Joshi P P, Mosconi E, Jones S C, Angelis F D and Zhu X Y 2017 *Sci. Adv.* **3** e1701217
[9] Cinquanta E, Meggiolaro D, Motti S G, Gandini M, Alcocer M J P, Akkerman Q A, Vozzi C, Manna L, Angelis F D, Petrozza A and Stagira S 2019 *Phys. Rev. Lett.* **122** 166601
[10] Evans T J S, Miyata K, Joshi P P, Maehrlein S, Liu F and Zhu X Y 2018 *J. Phys. Chem. C* **122** 13724
[11] Park M, Neukirch A J, Reyes-Lillo S E, Lai M, Ellis S R, Dietze D, Neaton J B, Yang P, Tretiak S and Mathies R A 2018 *Nat. Commun.* **9** 2525

[12] Puppin M, Polishchuk S, Colonna N, Crepaldi A, Dirin D N, Nazarenko O, De Gennaro R, Gatti G, Roth S, Barillot T, Poletto L, Xian R P, Rettig L, Wolf M, Ernstorfer R, Kovalenko M V, Marzari N, Grioni M and Chergui M 2020 *Phys. Rev. Lett.* **124** 206402

[13] Schilcher M J, Robinson P J, Abramovitch D J, Tan L Z, Rappe A M, Reichman D R and Egger D A 2021 *ACS Energy Lett.* **6** 2162

[14] Chen Y, Yi H T, Wu X, Haroldson R, Gartstein Y N, Rodionov Y I, Tikhonov K S, Zakhidov A, Zhu X Y and Podzorov V 2016 *Nat. Commun.* **7** 12253

[15] Neukirch A J, Nie W, Blancon J, Appavoo K, Tsai H, Sfeir M Y, Katan C, Pedesseau L, Even J, Crochet J J, Gupta G, Mohite A D and Tretiak S 2016 *Nano Lett.* **16** 3809

[16] Meggiolaro D, Ambrosio F, Mosconi E, Mahata A and Angelis F D 2019 *Adv. Energy Mater.* **10** 1902748

[17] Husanu M A, Vistoli L, Verdi C, Sander A, Garcia V, Rault J, Bisti F, Lev L L, Schmitt T, Giustino F, Mishchenko A S, Bibes M and Strocov V N 2020 *Commun. Phys.* **3** 62

[18] Huang K and Rhys A 1950 *Proc. R. Soc. A* **204** 406

[19] Huang K 1981 *Contemp. Phys* **22** 599

[20] Xu S J 2019 *Acta Phys. Sin.* **68** 2019 (in Chinese)

[21] Wang Z W, Sun Y, Cui Y, Xiao Y, Deng J P, Xiong W and Li Z Q 2021 *J. Phys.: Condens. Matter* **33** 145702

[22] Kartheuser E and Evrard R 1980 *Phys. Rev. B* **21** 648

[23] Matsuura M and Büttner H 1980 *Phys. Rev. B* **21** 679

[24] Cheng Z 1999 *Phys. Rev. B* **60** 15747

[25] Lin S H, Chang C H, Liang K K, Chang R, Shiu Y J, Zhang J M, Yang T S, Hayashi M and Hsu F C 2002 *Ultrafast Dynamics and Spectroscopy of Bacterial Photosynthetic Reaction Centers* (John Wiley and Sons, Inc.) pp. 8–9

[26] Devreese J T 2016 arXiv:1012.4576v6 [hep-ph]

[27] Quarti C, Grancini G, Mosconi E, Bruno P, Ball J M, Lee M M, Snaith H J, Petrozza A and Angelis F D 2014 *J. Phys. Chem. Lett.* **5** 279

[28] Brivio F, Frost J M, Skelton J M, Jackson A J, Weber O J, Weller M T, Goni A R, Leguy A M A, Barnes P R F and Walsh A 2015 *Phys. Rev. B* **92** 144308

[29] Iaru C M, Geuchies J J, Koenraad P M, Vanmaekelbergh D and Silov A Y 2017 *ACS Nano* **11** 11024

[30] Iaru C M, Brodu A, van Hoof N J J, ter Huurne S E T, Buhot J, Montanarella F, Buhbut S, Christianen P C M, Vanmaekelbergh D, Donega C de M, Rivas J G, Koenraad P M and Silov A Y 2021 *Nat. Commun.* **12** 5844

[31] Emin D 1999 *Polaron* (Cambridge University Press) p. 21

[32] Cui Y, Liu X Y, Ji S Y, Sun Y, Deng J P, Ma X F, Li Z Q and Wang Z W 2021 *J. Phys. Chem. Lett.* **12** 11182

[33] Wright A D, Verdi C, Milot R L, Eperon G E, Pérez-Osorio M A, Snaith H J, Giustino F, Johnston M B and Herz L M 2016 *Nat. Commun.* **7** 11755

[34] Sendner M, Nayak P K, Egger D A, Beck S, Müller C C, Epding B, Kowalsky W, Kronik L, Snaith H J, Pucci A and Lovrinčć R 2016 *Mater. Horiz.* **3** 613

[35] Wolf C, Kim J S and Lee T W 2017 *ACS Appl. Mater. Interfaces* **9** 10344

[36] Zheng F and Wang L W 2019 *Energy Environ. Sci.* **12** 1219

[37] Yin J, Li H, Cortecchia D, Soci C and Brédas J 2017 *ACS Energy Lett.* **2** 417

[38] Li S, Luo J, Liu J and Tang J 2019 *J. Phys. Chem. Lett.* **10** 1999

[39] Li J, Wang J, Ma J, Shen H, Li L, Duan X and Li D 2019 *Nat. Commun.* **10** 806

[40] Kandada A R S and Silva C 2020 *J. Phys. Chem. Lett.* **11** 3173

[41] Ivanovska T, Dionigi C, Mosconi E, Angelis F D, Liscio F, Morandi V and Ruani G 2017 *J. Phys. Chem. Lett.* **8** 3081

[42] Buizza L R V and Herz L M 2021 *Adv. Mater.* **33** 2007057

[43] Shi L and Wang L W 2012 *Phys. Rev. Lett.* **109** 245501

[44] Shi L, Xu K and Wang L W 2015 *Phys. Rev. B* **91** 205315

[45] Xiao Y, Wang Z W, Shi L, Jiang X W, Li S S and Wang L W 2020 *Sci. China Phys. Mech. Astron.* **63** 277312

[46] Kim K H, Jung J H and Noh T W 1998 *Phys. Rev. Lett.* **81** 1517

[47] Wang Z W, Xiao Y, Deng J P, Cui Y and Li Z Q 2019 *Phys. Rev. B* **100** 125308

[48] Cui Y, Xiao Y, Sun Y, Deng J P, Li Z Q and Wang Z W 2020 *J. Appl. Phys.* **128** 204302

[49] Bretschneider S A, Ivanov I, Wang H I, Miyata K, Zhu X and Bonn M 2018 *Adv. Mater.* **30** 1707312

[50] Joshi P P, Maehrlein S F and Zhu X 2019 *Adv. Mater.* **31** 1803054

[51] Kaur G, Babu K J, Ghorai N, Goswami T, Maiti S and Ghosh H N 2019 *J. Phys. Chem. Lett.* **10** 5302

[52] Zhu X Y and Podzorov V 2015 *J. Phys. Chem. Lett.* **6** 4758

[53] Thongnum A, Pingaew R and Pinsook U 2021 *Phys. Chem. Chem. Phys.* **23** 27320

[54] Frost J M 2017 *Phys. Rev. B* **96** 195202

[55] Motta C and Sanvito S 2018 *J. Phys. Chem. C* **122** 1361

[56] Thongum A and Pinsook U 2020 *Nanoscale* **12** 14112

[57] Brenner T M, Egger D A, Rappe A M, Kronik L, Hodes G and Cahen D 2015 *J. Phys. Chem. Lett.* **6** 4754

[58] Whitfield P S, Herron N, Guise W E, Page K, Cheng Y Q, Milas I and Crawford M K 2016 *Sci. Rep.* **6** 35685

[59] Liu L, Zhao R, Xiao C, Zhang F, Pevere F, Shi K, Huang H, Zhong H and Sychugov I 2019 *J. Phys. Chem. Lett.* **10** 5451

[60] Keshavarz M, Ottesen M, Wiedmann S, Wharmby M, Küchler R, Yuan H, Debroye E, Steele J A, Martens J, Hussey N E, Bremholm M, Roeffaers M B J and Hofkens J 2019 *Adv. Mater.* **31** 1900521

[61] Chen J, Messing M E, Zheng K and Pullerits T 2019 *J. Am. Chem. Soc.* **141** 3532

[62] Lee J W, Tan S, Seok S, Yang Y and Park N G 2022 *Science* **375** eabj1186